Accordion-like Actuators of Multiple 3D Patterned Liquid Crystal Polymer Films

Laurens T. de Haan, Vianney Gimenez-Pinto, Andrew Konya, Thanh-Son Nguyen, Julien M. N. Verjans, Carlos Sánchez-Somolinos, Jonathan V. Selinger, Robin L. B. Selinger, Dirk J. Broer,* and Albertus P. H. J. Schenning**

This work describes the fabrication, characterization, and modelling of liquid crystalline polymer network films with a multiple patterned 3D nematic director profile, a stimuli-responsive material that exhibits complex mechanical actuation under change of temperature or pH. These films have a discrete alternating striped or checkerboard director profile in the plane, and a 90-degree twist through the depth of the film. When actuated via heating, the striped films deform into accordion-like folds, while the film patterned with a checkerboard microstructure buckles out-of-plane. Furthermore, striped films are fabricated so that they also deform into an accordion shaped fold, by a change of pH in an aqueous environment. Three-dimensional finite element simulations and elasticity analysis provide insight into the dependence of shape evolution on director microstructure and the sample's aspect ratio.

1. Introduction

Stimuli-responsive materials have the ability to change their physical properties leading, for example, to the formation of complex shapes in response to an external stimulus. In many cases, such smart materials are prepared via assembly of components,[1,2] using two or more different constituent materials to induce folding. In organisms, by contrast, complex shape deformations are often driven by hierarchical structuring of molecular systems, such as the cellular ensembles forming muscles and the tissue of plants, which are capable of complex growth and movement.[3,4] In order to mimic such systems, stimuli-responsive materials must have a hierarchical structure that can be tailored to achieve a target actuation behavior, without the need to assemble separate mechanical components.[5] Previously, non-hierarchical programmable deformations of higher complexity, based on local swelling in water, have been shown in isotropic patterned cross-linked polymer gels.[6–9]

Liquid crystal polymer networks are another interesting class of stimuli-responsive actuators[10–14] which, in contrast to hydrogel-based actuators, also work in a solvent free environment. Such materials are fabricated by using reactive liquid crystalline molecules whose orientation can be manipulated using, for example, alignment layers and fixed by photopolymerization, resulting in hierarchical materials with a defined microstructure over macroscopic length scales. The average alignment direction of the liquid crystalline molecules is called the director, and the magnitude of orientational order of molecular orientation is described by a scalar order parameter S.[15] In a liquid crystal polymer network, the material stretches or shrinks anisotropically along the director orientation as the order parameter changes, for instance due to change of temperature or chemical environment. So far, reported liquid crystalline polymer networks include samples with a unidirectional alignment so they contract in the direction parallel to the alignment director upon application of a stimulus.[16] Other reported films have a molecular director that varies through the depth, that is, twisted nematic and splayed configurations; these samples bend[17–21] or curl[22,23] when a stimulus is applied.[24] Recently, we and others have reported more exotic deformations of liquid crystal polymer films, with a circular director profile in the plane of the polymer film. These samples showed deformation into cone and anti-cone shapes upon heating.[25,26] There the director microstructure was uniform through the sample thickness and thus essentially two-dimensional. More complex reversible deformation can be achieved by imposing a three-dimensional director profile on the film, with variation through the thickness as well as in the plane of the polymer film. For instance, recently shape-memory materials have been reported with alternating twisted nematic and monodomain sections.[27]

L. T. de Haan, J. M. N. Verjans, Prof. D. J. Broer, Dr. A. P. H. J. Schenning
Functional Organic Materials and Devices
Department of Chemical Engineering and Chemistry
Eindhoven University of Technology
Den Dolech 2, 5600, MB Eindhoven, The Netherlands
E-mail: D.Broer@tue.nl; A.P.H.J.Schenning@tue.nl
V. Gimenez-Pinto, A. Konya, T. S. Nguyen, Prof. J. V. Selinger, Prof. R. L. B. Selinger
Chemical Physics Interdisciplinary Program
Liquid Crystal Institute
Kent State University
Kent, OH, 44242, USA
E-mail: rselinge@kent.edu
Dr. C. Sánchez-Somolinos
Instituto de Ciencia de Materiales de Aragón
Departamento de Física de la Materia Condensada
CSIC-Universidad de Zaragoza,
Zaragoza, Spain

DOI: 10.1002/adfm.201302568

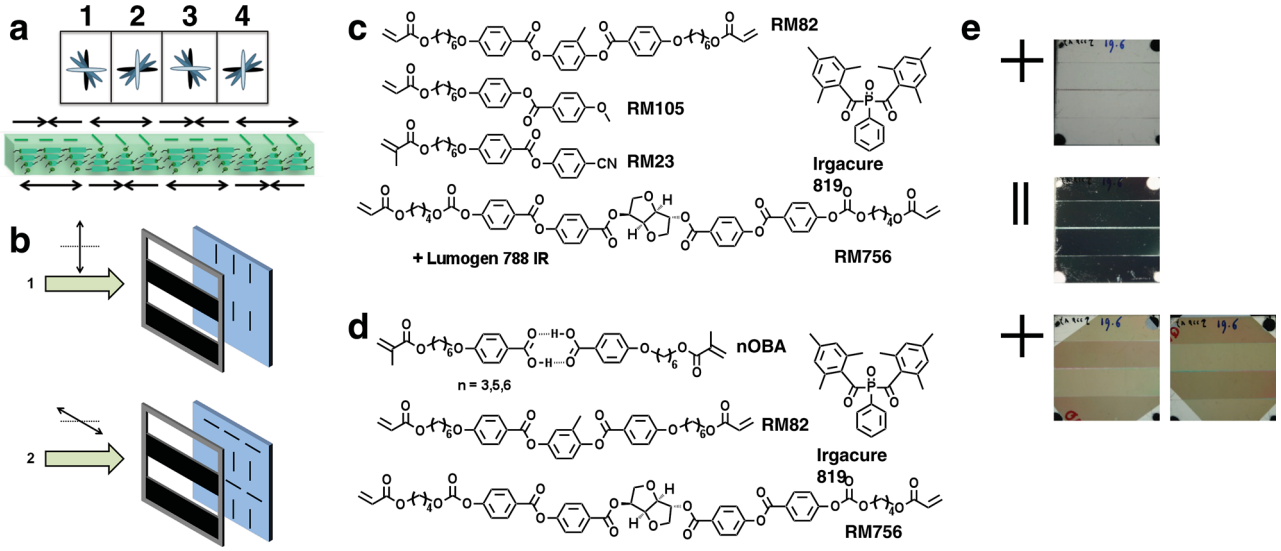

Figure 1. a) Alignment pattern of the accordion-shaped actuator, top view and side view. Arrows indicate the contraction and expansion directions along the length of the film. Each domain is 5 mm wide and 7.5 mm long. b) Two-step procedure for the preparation of the alignment layers. The black arrows indicate the polarization direction of the UV light. Before the second exposure step the polarization of the light is rotated 90 degrees while the sample is rotated 180 degrees. c) Liquid crystal mixture used to make a heat responsive actuator (RM82:RM105:RM23 = 2:3:1), including an IR absorber (Lumogen 788 IR), a radical initiator, and a chiral dopant (RM756). d) Liquid crystal mixture used to make a pH responsive polymer actuator (3OBA:5OBA:6OBA = 1:1:1, RM82 12 w%), including the initiator and chiral dopant. e) Optical analysis of a four-lane alternating twisted nematic actuator. The film was analyzed between crossed polarizers (top) and parallel polarizers (middle). To show the difference in orientation between the lanes, it was also viewed between crossed polarizers with a quarter wave plate on top of the sample in two different orientations (bottom).

In this work, we have prepared patterned liquid crystal actuators with a three-dimensional director variation. These films have a discrete alternating striped or checkerboard director profile in the plane and a 90-degree twist through the depth of the film. These samples show complex reversible deformation driven by their director profile. Upon heating, the striped samples undergo a reversible transition from a long flat ribbon to a bent/folded state resembling an accordion fold, and therefore achieve a large lateral displacement between the endpoints of the film. The actuators with the checkerboard pattern of twist domains buckle out-of-plane. We also show that accordion-like deformation can be achieved in an aqueous environment by striped patterned polymer actuators that respond to pH changes. Finally, finite element analysis predicts the observed deformations for both types of actuators and shows the importance of the aspect ratio of the 3D pattern in the polymer samples.

2. Results and Discussion

To induce accordion fold actuation, the nematic director field was patterned in discrete stripes with twisted nematic director of alternating orientation (**Figure 1**a). Stripes 1 and 3 have the director at the top surface oriented along the film's long axis, while the director at the bottom surface is oriented along the film's short axis. Stripes 2 and 4 have the director at the top surface oriented along the film's short axis and the director at the bottom surface oriented along the film's long axis. These boundary conditions lead to a 90° twist across the depth of the film. The twist in all stripes has uniform handedness, induced by the addition of a trace amount of chiral dopant as described below. When heated, the material in each stripe expands along the film's long axis on one side and contracts in the same direction on the other side (Figure 1a). Therefore, the stripes are expected to bend in opposite directions upon actuation to form accordion-style folds. The actuators were prepared according to a similar procedure as described previously,[25] by photopolymerizing a liquid crystal mixture confined between two substrates with patterned alignment layers that impose anchoring forces on the liquid crystal's nematic director field. For the preparation of the required alignment layers, we used a thin film of a linearly photopolymerizable polymer (LPP) spincoated onto glass substrates. When irradiated with linearly polarized UV light, the LPP forms an alignment layer with the aligning director oriented parallel to the polarization direction of the UV light. A laned photomask was used to create the desired pattern using two irradiation steps. First, the substrate was irradiated with polarized UV light through the photomask. Then the substrate was rotated to expose the previously unexposed parts, and the second exposure was carried out with the polarization direction of the light rotated by 90 degrees (Figure 1b). To obtain an alignment cell, two substrates were glued together with a small gap between them. Care was taken to superimpose the substrates with the alignment directors in an orthogonal position, to ensure a twisted nematic conformation of the liquid crystals. A mixture of polymerizable liquid crystals was used as described in earlier work ($T_g \approx 45$ °C),[25] which contains a photoinitiator (Irgacure 819) to initiate the polymerization, and an IR absorber in order to improve the response of the material to IR heating (Figure 1c). The cells were filled in the isotropic phase and, after cooling the liquid crystalline samples to the

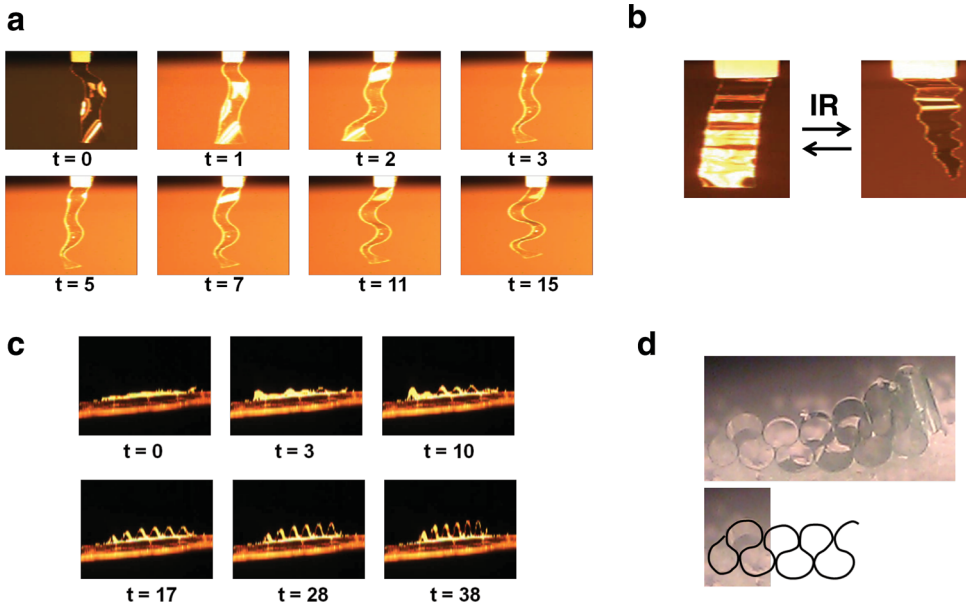

Figure 2. a) Deformations of the actuator (aspect ratio 1650 : 275 :1) upon irradiation with an IR source for time *t* in seconds after switching on the light. b) Deformation of a 12-lane patterned film, while being held vertically in front of the IR source. c) Deformation of a 12-lane patterned film, while lying horizontally on a surface. d) Fully contracted "teardrop" state of the twelve-lane polymer actuator. In the bottom picture, a line drawing of the teardrop folds is overlaid on a section of the photograph for increased clarity.

nematic phase, photopolymerization was carried out to obtain a polymer film in which the alignment director of the liquid crystals was fixed.

After retrieving the film from the alignment cell, it was optically analyzed by placing it between linear polarizers (Figure 1e). Twisted nematic liquid crystals rotate the polarization direction of linearly polarized light by 90 degrees, causing the film to be bright between crossed polarizers and dark between parallel polarizers. Furthermore, when the film was placed between crossed polarizers with a quarter wave plate on top of the sample at a 45 degrees angle, a difference in brightness between the domains was observed. This is explained by the slow axis of the wave plate being either parallel or perpendicular to the midplane director of the nematic twist, which adds to the optical retardation or compensates for it, respectively. The sample was more closely investigated using polarized optical microscopy, and was found to contain no significant defects aside from the narrow lines between the patterned domains, which are caused by a slight mismatch of the alignment layers. These lines are expected not to influence the deformation behavior of the actuators. Surface profilometry and interferometry were used to measure the final thickness of the film, which was found to be 12–19 μm (see Supporting Information for details).

To perform the actuation experiments, a strip of 30 mm × 5 mm was cut from the freestanding film, which resulted in an aspect ratio of roughly 1650 : 275 :1. The films were clamped on their short end and actuated through heating by exposure to an IR source. It should be noted that in all cases, the film was already slightly bent before heating was applied. This initial bend is probably due to stresses induced during the photopolymerization of the material at elevated temperatures in the flat state. Upon cooling down to room temperature, the anisotropy of the system increases, which may have caused the material to deform. Upon heating the vertically positioned film, the four areas of the film deformed by bending in opposite directions. We clearly observed a four-bend accordion shape (**Figure 2**a, Movie S1, Supporting Information), although the deformation of the area closest to the clamp is somewhat suppressed. The deformation reversed upon switching off the IR source, and the speed and magnitude of the deformation could be influenced by varying the intensity of the IR irradiation.

The experiment was repeated for a 12-lane film of the same dimensions. This film was both actuated while being held vertically in front of the IR source (Figure 2b, Movie S2, Supporting Information) and while lying horizontally on a glass surface (Figure 2c, Movies S3,S4, Supporting Information). Again, the accordion shape was observed with the correct number of bends, but the amplitude was smaller compared to the four-lane actuator. Interestingly, upon heating the film on the surface, sharp folds were observed (Figure 2 at t = 38 s). One explanation for this is that due to the tips of the waves receiving more direct IR irradiation, these areas have a higher temperature and bend more sharply. However, the effect was not observed in the vertical experiments, and might also be caused by friction between the sample and the glass substrate. In addition to the expected shape change, a secondary deformation was observed in both experiments involving the twelve-lane actuator. In the vertical experiment, a right-handed twist over the entire length of the film was observed (Figure 2b), while in the horizontal experiment a sideways bending deformation took place. These two observations are probably different manifestations of the same effect, which might be related to the twist handedness of the twisted nematic moieties. Finally, it was found that if the actuator was heated above a certain point it showed a strong

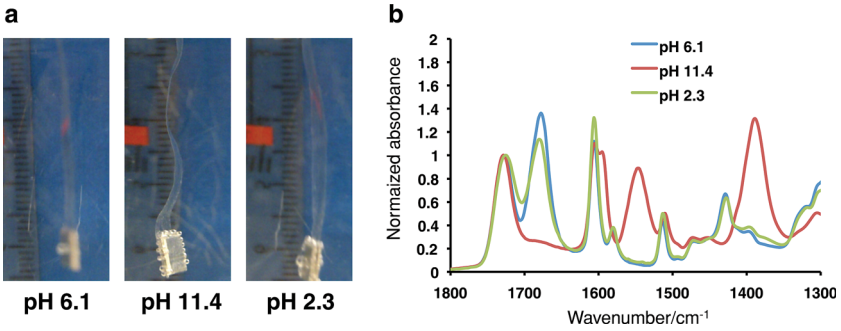

Figure 3. a) Deformation of a pH responsive alternating twisted nematic actuator. The film is flat at pH 6, and obtains the accordion shape when the pH is increased to 11. When the pH is then reduced to 3, the flat shape is recovered. b) Normalized FTIR spectra of the pH responsive film at various stages during the experiment. The peak at 1682 cm^{-1} correspond to the C=O stretching in hydrogen bonded dimers, while the peaks at 1547 and 1395 cm^{-1} are from antisymmetric and symmetric COO^- stretching, respectively.[29]

contraction, and the folds obtained a "teardrop" shape, resulting in an overall shape not unlike a so-called "ruff collar"[28] (Figure 2d, Movie S5, Supporting Information). No further deformation was observed after this shape was obtained.

To show that this exotic type of deformation can also be induced by other stimuli, an actuator was prepared which responds to changes in the pH of an aqueous environment. To this end, a reactive mesogen mixture with internal hydrogen bonds[29] (Figure 1d) was used to make the liquid crystal network. Upon immersion of the film in a basic solution, the internal hydrogen bonds are converted into a carboxylic salt.[28] This causes an anisotropic swelling in all directions, having a larger expansion in the direction perpendicular to the alignment director.[29] A ribbon of freestanding film with four domains of alternating twisted alignment, prepared using the same alignment cells as used before (Figure 1b), was immersed in demineralized water, with a 40 mg metal weight attached to the far end to keep the film from floating to the surface or crumpling up against the clamp (**Figure 3**a). The pH of the medium was monitored using a pH meter, and was determined to be 6.1 for demineralized water. Also, the FTIR spectrum of the material was recorded prior to the experiment to keep track of the presence of the internal hydrogen bonds (Figure 3b). A 0.1 M KOH solution was added to increase the pH of the environment to 11.4. At this pH the internal hydrogen bonds of the network were converted to the corresponding carboxylic potassium salt, which was confirmed in the FTIR spectrum. The induced hygroscopic behavior in the material caused it to take up water from the aqueous medium, which in turn caused a decrease in anisotropy, and an accordion shape was observed (Figure 3a). As observed before, the bends close to the clamped end were somewhat suppressed, but the middle regions were bending as programmed. After being exposed to the basic solution, the curvature of the bending domains no longer increased, and the activation process was considered complete. At this stage, four bends could be identified, which corresponded with the four alignment domains. This bending is less pronounced when compared to the heat responsive actuators, both due to the presence of a weight on one end of the film and due to the fact that the anisotropic swelling takes place in all directions of the film.[29] The pH was decreased to 2.3, which resulted in the recovery of the hydrogen bonds and the FTIR spectrum reverted back to show the original peaks. As expected, the film returned to its original flat shape.

To examine the mechanism driving these shape transformations, we carried out a finite element elastodynamics analysis. We meshed thin film samples in three dimensions, rather than treat them as having infinitesimal thickness. Our Hamiltonian-based model includes the system's kinetic energy, elastic energy, and coupling between strain and nematic order; further details of the finite element model are provided in the Supporting Information. The scalar order parameter at the time the material is cross-linked is defined by the parameter S_o. As the temperature increases, the nematic order parameter S decreases, inducing a contraction of the sample along the n_i direction and an elongation in the two directions perpendicular to n_i. Thus, a non-uniform director field within the sample produces non-uniform internal strains as the temperature changes, giving rise to complex shape evolution. We assume that the director field n_i is strongly anchored by cross-linking of the polymer network such that it rotates with the body but does not otherwise reorient in response to strain. This is the characteristic behavior of a nematic glass, and is a reasonable approximation for this experimental system below its glass transition temperature and where there is no external applied mechanical stress. In previous work, we have also considered the case where the director field is less strongly anchored.[30]

To represent a change of temperature, the scalar order parameter S was raised (to represent cooling) or lowered (to represent heating) gradually and was then held fixed until the sample reaches elastic equilibrium. We show a finite element simulations of a sample with aspect ratio 50:10:1 and with stripe widths of different sizes (**Figure 4**a,b), starting with a sample with four stripes of alternating twist orientation (Figures 1a, 4a). As temperature increased, we observed formation of undulations with two crests and two valleys. The handedness of the director twist induced a slight chiral bend within each stripe; as a result we observed a small zigzag deformation along the sample borders. We repeated this simulation for a sample of the same aspect ratio, divided into 8 stripes (Figure 4b). We carried out simulations for samples with 2 to 12 stripes, keeping the sample aspect ratio constant, and found that larger stripe width drives larger undulation amplitude (Figure 4c). This is consistent with the experimental finding that a 4-lane actuator shows larger amplitude compared to a 12-lane actuator.

For a large enough stripe width to thickness ratio, we observed a transition from a sinusoidal undulation to the formation of teardrop-shaped accordion folds, as shown in (Figure 4d). The central axis of the ribbon formed approximately circular arcs of alternating orientation. Finite element simulation also predicted that the ribbon flexes across its short axis with negative Gaussian curvature, with orientation alternating along each circular arc. We also observed slight out-of-plane twist similar to that seen in the practical experiments (Figure 2b).

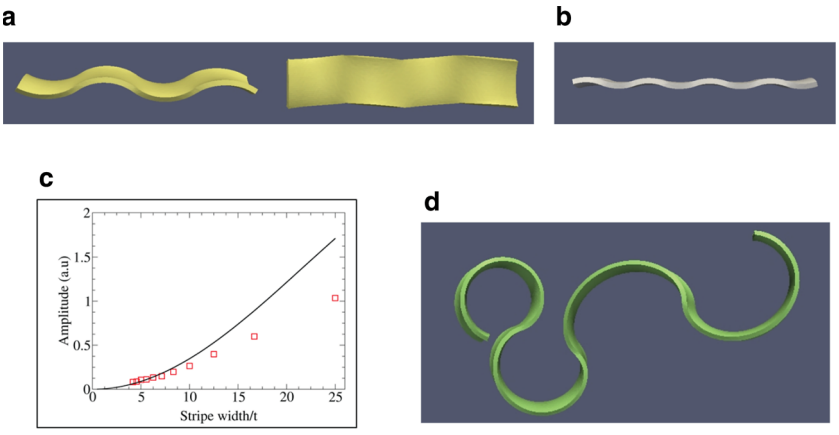

Figure 4. Finite element simulation of the shape deformation of a nematic network with alternating twisted domains when its nematic order decreases on heating. For stripe width/thickness ratio in the range of 4–25, we observe smooth, sinusoidal deformation; a) four stripes (ratio = 12.5) and b) eight stripes (ratio = 6.25). c) Amplitude of resulting undulations increases as a function of stripe width/thickness ratio; solid line represents the analytical prediction and square points are simulation data. d) Simulation of a longer sample with stripe width/thickness ratio = 50 and a larger temperature change ($\Delta S = -0.8$) shows formation of teardrop-shaped accordion folds.

Using a simple analytical model, we estimated the undulation amplitude as a function of stripe width, which is plotted together with simulation data in Figure 4c. Here we assumed that each stripe forms a circular arc with curvature κ, and the entire sample consists of several circular arcs joined together. Details of this calculation are included in the supplementary information. Analytical prediction agreed with the finite-element simulations of the amplitude for small stripe width but overestimated the amplitude for wider stripes; presumably the discrepancy arises because the true deformation is not just a circular arc but involves a more complex distortion with negative Gaussian curvature. We also used this simple mathematical model to estimate the energetics involved with the deformation. As the film curves, it contracts from the initial length L_0 to the final length $= \frac{2L_0}{w\kappa}\sin\frac{w\kappa}{2}$, where w is the stripe width. To calculate the maximum work that can be done by this contraction, we compared the energy of the curved state with the energy of the flat state at the same ΔS. This comparison shows that the maximum work is $W_{max} \approx \frac{3\pi^2\alpha^2\Delta S^2 V}{64(8\mu+\alpha\Delta S)} \approx \frac{(\kappa d)^2 E V}{18}$, where V is the volume, d the thickness, and $E = 3\mu$ the Young's modulus of the material. For the experimental sample, we estimated the dimensions 30 mm × 5 mm × 15 μm, the Young's modulus $E = 1$ GPa (below the glass transition), and the curvature $\kappa = 1/3$ mm^{-1}. Hence, we estimate the maximum work that can be done by contraction as $W_{max} \approx 3 \times 10^{-6}$ J. For comparison, the mass of the sample is approximately 3×10^{-6} kg, so W_{max} is about three times the work needed to lift its own mass by its own length. This quantity could be increased through optimization of actuator geometry, and by altering the material's composition and processing to increase the strength of coupling between strain and orientational order, characterized by the parameter α.

To extend our fabrication method to an even more complex deformation, an actuator was prepared with two orthogonally superimposed lane masks to make a checkerboard pattern.[31] Four irradiation steps were required, while rotating the substrate 90 degrees after each step, to expose the whole substrate area (**Figure 5**a). Again, an alignment cell was prepared and filled with the mixture of reactive mesogens (Figure 1b), which was cured through UV irradiation, producing a director pattern with twisted domains (Figure 5a). After removal of the film from the cell (23 mm × 23 mm, aspect ratio roughly 1810 : 1810 : 1), the actuation experiment was carried out for the checkerboard film (Figure 5b, Movie S6, Supporting Information). Upon heating, the film deformed from a mostly flat shape to form a periodic square pattern of peaks, depressions, and saddle points. Like the 12-lane accordion, a deformation over the entire surface of the film was observed. The corners of the film bent inwards to give the film an overall dome-shaped structure.

To gain an understanding of this actuation pattern, we performed a finite element analysis simulation of a 3 × 3 checkerboard actuator, displayed in **Figure 6**, showing shape evolution with increasing temperature. We used a mesh with aspect ratio of 50 : 50 : 1. The sample distorts into an arrangement of peaks, depressions, and saddle points corresponding with the square domains. The simulation also shows an overall dome-shape superposed over the smaller wavelength undulation, in agreement with experimental findings.

3. Conclusions

We have demonstrated a new family of actuators with a 3D-patterned structure that show exotic deformations. Our results show that exciting new deformations in liquid crystal actuators can be achieved by 3D structuring and we expect that many

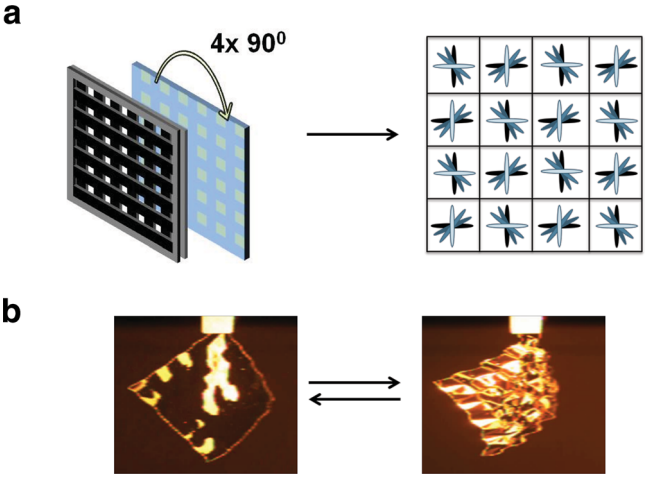

Figure 5. a) Preparation procedure of the checkerboard alignment layers, and top view of the final pattern (only 4 × 4 squares shown) b) Deformation upon IR heating of a film with a checkerboard pattern (aspect ratio 1810 : 1810 : 1).

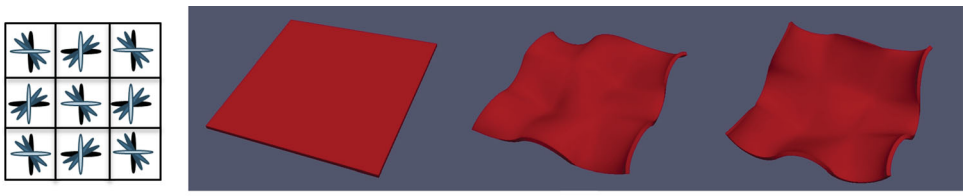

Figure 6. a) Top view of the director microstructure of a 3 × 3 checkerboard actuator. b) Finite element simulation of the 3 × 3 checkerboard actuator when heated to the isotropic state.

new shapes will be developed in the near future. This could eventually lead to new ways to perform auto-origami in plastic materials. The striped actuators showed accordion-like deformations upon application of an appropriate stimulus, which, depending on the chosen chemical composition of the mixture of reactive mesogens, could either be a temperature or a pH variation. This kind of out of plane actuation achieves a larger total displacement for a given temperature change than could be accomplished by contracting a monodomain sample of the same material with uniform nematic director. We also show that these deformations can be predicted with a mathematical simulation based on finite element analysis showing the importance of the aspect ratio of the 3D pattern in polymer films. The calculations also show that the strength of the actuators is limited, and better materials are required. For instance, side-on[32] or mainchain[33] liquid crystal polymer networks could be used. Simulations of this type, validated by suitable experiments, will be of value in engineering complex actuator geometries in future applications. Such actuators are potentially useful in applications where large, complex displacements are valued above strength and power. Applications could range from moving elements in microfluidic systems, such as shutters and flow controllers, to medical systems and microrobotics, where precisely controlled, complex movements are desired.

4. Experimental Section

Materials: All materials were used as received from Merck (RM82, RM105, RM23), Philips Research Organics (3-OBA, 6-OBA), Synthon Chemicals (5-OBA), BASF (Lumogen 788 IR, LC756), Ciba Specialty Chemicals (Irgacure 819), Rolic (ROP-108), and Aldrich (t-butyl hydroquinone, dichloromethane). The alignment cells were prepared using 18 micrometer SP-218 Micropearl plastic spacers (Sekisui Chemical Co.).[25]

Layers of the photoalignment material (ROP-108) were spincoated onto glass substrates using a Karl Suss RC8 spincoater. Photoalignment was carried out using an Ominicure S2000 UV lamp. A Newport 10LP-UV precision linear polarizer, mounted in a Thorlabs PRM1/MZ8 rotation mount, was used to polarize the UV light in various directions, and the substrate was rotated using a Thorlabs CR1/M-Z7 rotation stage (irradiation intensity ≈13 mW cm^{-2} in the UVA range). The rotation of the polarizer and stage was controlled with Thorlabs TDC001 controllers, which were programmed with APT software. Photopolymerization of the liquid crystal mixtures was carried out using an Omnicure S2000 UV lamp with 320–500 nm filter (≈25 mW cm^{-2}). To remove the alignment material from the surface of the pH-responsive actuators, an Emitech K1050X plasma asher was used.

The thickness of the actuator films was measured using both a Fogale nanotech zoomsurf 3D interferometer and a Veeco Dektak 150 surface profilometer. Slide-on ATR IR spectra of the pH-responsive films were recorded using a Varian 670 FTIR spectrometer. For the IR actuation experiments, a Heraeus Noblelight Shortwave surface irradiator (type "Duo", 250 Watt, 57.5 Volt) with gold reflector was used. During the pH experiments, the pH of the solution was monitored using an inoLab pH meter.

Preparation of Alternating Twisted Alignment Cells: 3 cm × 3 cm glass plates were cleaned with ethanol. ROP-108 was spincoated onto the plates at 1500 RPM for 30 s. The plates were heated briefly to 115 °C to evaporate the solvent. Irradiation of each LPP substrate was carried out through a photomask with polarized UV light for 50 s. When a 4- or 12-lane pattern was prepared, two irradiations were carried out on each substrate. After the initial irradiation step, the substrate was rotated 180 degrees to expose the non-irradiated areas, while the polarizer was rotated 90 degrees, and a second irradiation was carried out. When a chessboard pattern was prepared, the substrates were irradiated four times and rotated 90 degrees between each irradiation step. In all cases, the plates were glued into cells, using 18 micron plastic spacers to secure the cell gap. Care was taken to glue the cells in an orthogonal fashion to obtain cells that force the LC material into a twisted nematic conformation.

Preparation of Heat-Responsive, Alternating Twisted Nematic Actuators: RM82 (201.1 mg), RM105 (302.2 mg), and RM23(101.5 mg) were put into a screw-cap vial. A 1.5 mg mL^{-1} solution of the thermal inhibitor tert-butyl hydroquinone and the chiral dopant LC756 in CH_2Cl_2 was added (≈90 µL), as well as the radical initiator Irgacure 819 (3.3 mg) and the IR absorber Lumogen 788 IR (0.8 mg). The components were dissolved in CH_2Cl_2, which was then evaporated by stirring the solution at 80 °C. An alignment cell was brought to 80 °C, and the cell gap was filled with the mixture though capillary action. When the cell was completely filled, it was cooled down slowly to 60 °C. Then UV polymerization took place in the nematic phase by UV irradiation for 5 min. Finally, the cell was opened to retrieve the freestanding polymer film. The film thickness was measured using surface profilometry and interferometry (see Supporting Information, Table S1).

Preparation of pH-Responsive, Alternating Twisted Nematic Actuators: 3-OBA (99.5 mg), 5-OBA (99.8 mg), 6-OBA (99.9 mg), RM82 (42.2 mg), and Irgacure 819 (6.9 mg) were put into a screw-cap vial. Tert-butyl hydroquinone (0.071 mg) and LC756 (0,35 mg) were added as a solution in CH_2Cl_2. The components were dissolved in CH_2Cl_2, the resulting solution was stirred while heating with a heat gun, and the solution was vortex-stirred for 5 min. The solvent was removed by heating the solution to 30 °C under argon flow, followed by drying in vacuo for one hour. An alignment cell was brought to 90 °C, and the cell gap was filled with the mixture though capillary action. When the cell was completely filled, it was cooled down slowly to 80 °C. Then UV polymerization took place by UV irradiation for 5 min. Finally, the cell was opened to retrieve the freestanding film.

Investigation of IR Actuation: Strips were cut from the alternating twisted nematic films. The following dimensions were used: 4-lane and 12- lane actuator: 30 mm × 5 mm, chessboard actuator: 23 mm × 23 mm. The films were actuated either in the vertical or horizontal position. When actuating in the vertical position, they were held with a tweezers in front of the IR lamp until actuation took place.

When horizontal actuation was required, the actuator was placed on a glass slide which was covered with sand to reduce friction. The material was then irradiated from above.

Investigation of pH Actuation: The film was subjected to oxygen plasma ashing for 4 min at 45 Watt to remove any remaining alignment material from the surface. An IR spectrum of the film was measured, and a 40 mg weight was attached to one end. The film was immersed in demineralized water, which was brought to pH 11.4 by slowly adding a 0.1 M KOH solution, and kept at that level for 17 min. The film was removed from the medium, dried, and an IR spectrum was recorded. The film was placed back, and the pH was decreased to 2.3 by the slow addition of a 1 M HCl solution. The film was removed from the medium, dried, and an IR spectrum was recorded.

Finite Element Elastodynamics Simulation: In order to implement finite element elastodynamic simulations, each thin film sample is discretized into an unstructured 3D tetrahedral mesh. Meshes were generated using Salome.[34] In Figures 4a-c, we used a mesh of aspect ratio 50-10-1 with 66 647 tetrahedra and 14 274 nodes. In figure 4d we used a mesh of aspect ratio 200-10-1 with 270 549 tetrahedra and 52 850 nodes.

The sample stripe width/thickness ratio in our experimental studies was approximately 130. However due to hardware limitations, the largest stripe width/thickness ratio we could achieve via simulation was 50, considering the size of the required mesh. This ratio was sufficiently high to drive formation of teardrop-shaped accordion folds. The checker board actuator was modeled using a mesh of aspect ratio 50-50-1 with 268 246 tetrahedra and 52 780 nodes (Figure 6).

Our 3D finite element elastodynamics code was developed in-house and runs in a GPU computing environment. The algorithm is based on the Hamiltonian:

$$H = \frac{1}{2}\sum m_p v_p^2 + \frac{1}{2}\sum V^t C_{ijkl}\varepsilon_{ij}^t\varepsilon_{kl}^t - \alpha\sum_t^p V^t\varepsilon_{ij}^t\,(S(T)^t - S_0)\frac{1}{2}\left(3n_i^t n_j^t - \delta_{ij}\right)$$

The first term describes kinetic energy, calculated as a sum over nodes p where the mass m_p of each node is determined using the lumped mass approximation,[7] and v_p is the node's instantaneous velocity. The second term represents the elastic energy of the sample, summed over all the tetrahedral elements t. Here C_{ijkl} is the elastic stiffness tensor,[8] assumed to be uniform, and ε_{ij} is the Green-Lagrange nonlinear strain tensor, which is defined in the body frame of the element.[9] This form of elastic strain energy function is unchanged by simple rotations of the sample. The third term represents the coupling between strain and nematic order of the liquid crystal. The nematic director $n_i(r)$ is treated as piece-wise constant within each tetrahedral element; mechanical strain ε is calculated with respect to the reference state of the sample at the time of cross-linking; the scalar order parameter at the time the material is cross-linked is defined by the parameter S_o. We simulated temperature change by adjusting the scalar order parameter S.

The effective force on each node is calculated as the derivative of the potential energy of the system with respect to the node's displacement, with a contribution from each volume element touching the node. The system evolves via $F = ma$ dynamics; we integrate the equations of motion using the velocity Verlet algorithm. We apply dissipative forces proportional to the node momentum, enabling the sample to relax to elastic equilibrium after the initial change in the nematic order parameter S.

We model the accordion deformation assuming that each stripe forms a circular arc with curvature κ, as a result the entire sample consists of several circular arcs joined together. We calculate the strain tensor ε_{ij} for this deformation, under the constraint of incompressibility. We then minimize the elastic energy

$$H_E = \int d^3r\,\left[\mu\varepsilon_{ij}\varepsilon_{ij} - \alpha\varepsilon_{ij}\Delta S\frac{1}{2}\left(3n_i n_j - \delta_{ij}\right)\right]$$

where μ is the shear modulus and α the coupling between strain and orientational order.

At the minimum, the curvature becomes

$$\kappa = \frac{3\pi\alpha\Delta S}{2d\,(8\mu + \alpha\Delta S)}$$

where d is the thickness of the film. The resulting amplitude of the deformation is

$$A = \frac{4}{\kappa}\sin^2\left(\frac{w\kappa}{4}\right)$$

where w is the stripe width.

Supporting Information

Supporting Information is available from the Wiley Online Library or from the author.

Acknowledgements

L.T.H. and V.G.-P. contributed equally to this work. The authors are grateful to the Netherlands Organization for Scientific Research (NWO, VICI grant), the Spanish MINECO project (MAT2011-27978-C02-02), the CSIC project (i-LINK0394), Gobierno de Aragon, and FEDER funding (EU) for their financial support. Work supported by NSF-DMR 1106014; computing resources provided by the Ohio Supercomputer Center (V.G.-P., A-K, J.S., R.S).

Received: July 30, 2013
Revised: August 28, 2013
Published online: October 30, 2013

[1] E. Hawkes, B. An, N. M. Benbernou, H. Tanaka, S. Kim, E. D. Demaine, D. Rus, R. J. Wood, *Proc. Natl. Acad. Sci. U. S. A.* **2010**, *107*, 12441.
[2] N. Bassik, G. M. Stern, D. H. Gracias, *Appl. Phys. Lett.* **2009**, *95*, 3.
[3] M. J. Harrington, K. Razghandi, F. Ditsch, L. Guiducci, M. Rueggeberg, J. W. C. Dunlop, P. Fratzl, C. Neinhuis, I. Burgert, *Nat. Commun.* **2011**, *2*, 337.
[4] Y. Forterre, J. M. Skotheim, J. Dumais, L. Mahadevan, *Nature* **2005**, *433*, 421.
[5] T. Aida, E. W. Meijer, S. I. Stupp, *Science* **2012**, *335*, 813.
[6] G. Stoychev, S. Turcaud, J. W. C. Dunlop, L. Ionov, *Adv. Funct. Mater.* **2013**, *23*, 2295.
[7] H. L. S. Thérien-Aubin, Z. L. Wu, Z. Nie, E. Kumacheva, *J. Am. Chem. Soc.* **2013**, *135*, 4834.
[8] J. Kim, J. A. Hanna, M. Byun, C. D. Santangelo, R. C. Hayward, *Science* **2012**, *335*, 1201.
[9] P. Dayal, O. Kuksenok, A. C. Balazs, *Soft Matter* **2010**, *6*, 768.
[10] M. Warner, E. M. Terentjev, *Liquid Crystal Elastomers*, Oxford University Press, Oxford, UK **2003**.
[11] H. Finkelmann, S. T. Kim, A. Munoz, P. Palffy-Muhoray, B. Taheri, *Adv. Mater.* **2001**, *13*, 1069.
[12] C. Ohm, M. Brehmer, R. Zentel, *Adv. Mater.* **2010**, *22*, 3366.
[13] D. J. Broer, G. P. Crawford, S. Zumer, *Cross-linked Liquid Crystalline Systems*, CRC Press, Boca Raton, FL, USA, **2011**.
[14] Y. L. Yu, M. Nakano, T. Ikeda, *Nature* **2003**, *425*, 145.
[15] A. Jakli, A. Saupe, in *One- and Two-Dimensional Fluids: Properties of Smectic, Lamellar and Columnar Liquid Crystals (Condensed Matter Physics)*, Taylor & Francis, Boca Raton, FL, USA **2006**, 352.
[16] H. Wermter, H. Finkelmann, *e-Polymers* **2001**, *13*, 1.
[17] K. D. Harris, C. W. M. Bastiaansen, D. J. Broer, *Macromol. Rapid Commun.* **2006**, *27*, 1323.

[18] G. N. Mol, K. D. Harris, C. W. M. Bastiaansen, D. J. Broer, *Adv. Funct. Mater.* **2005**, *15*, 1155.
[19] C. L. van Oosten, C. W. M. Bastiaansen, D. J. Broer, *Nat. Mater.* **2009**, *8*, 677.
[20] S. Serak, N. Tabiryan, R. Vergara, T. J. White, R. A. Vaia, T. J. Bunning, *Soft Matter* **2010**, *6*, 779.
[21] M. Moua, R. R. Kohlmeyer, J. Chen, *Angew. Chem. Int. Ed.* **2013**, *52*, 9234.
[22] M. H. Godinho, J. P. Canejo, G. Feio, E. M. Terentjev, *Soft Matter* **2010**, *6*, 5965.
[23] Y. Sawa, F. F. Ye, K. Urayama, T. Takigawa, V. Gimenez-Pinto, R. L. B. Selinger, J. V. Selinger, *Proc. Natl. Acad. Sci. U. S. A.* **2011**, *108*, 6364.
[24] Complex deformation in liquid crystalline networks can also be achieved by applying a localized stimulus, see: a) M. Camacho-Lopez, H. Finkelmann, P. Palffy-Muhoray, M. Shelley, *Nat. Mater.* **2004**, *3*, 307; b) M. Yamada, M. Kondo, J.-i. Mamiya, Y. Yu, M. Kinoshita, C. J. Barrett, T. Ikeda, *Angew. Chem. Int. Ed.* **2008**, *47*, 4986; c) M. Yamada, M. Kondo, R. Miyasato, Y. Naka, J.-i. Mamiya, M. Kinoshita, A. Shishido, Y. Yu, C. J. Barrett, T. Ikeda, *J. Mater. Chem.* **2009**, *19*, 60.
[25] L. T. de Haan, C. Sanchez-Somolinos, C. M. W. Bastiaansen, A. P. H. J. Schenning, D. J. Broer, *Angew. Chem. Int. Ed.* **2012**, *51*, 12469.
[26] M. E. McConney, A. Martinez, V. P. Tondiglia, K. M. Lee, D. Langley, I. I. Smalyukh, T. J. White, *Adv. Mater.* **2013**, DOI: 10.1002/adma.201301891.
[27] K. M. Lee, T. J. Bunning, T. J. White, *Adv. Mater.* **2012**, *24*, 2839.
[28] M. M. Muller, M. Ben Amar, J. Guven, *Phys. Rev. Lett.* **2008**, *101*, 4.
[29] K. D. Harris, C. W. M. Bastiaansen, J. Lub, D. J. Broer, *Nano Lett.* **2005**, *5*, 1857.
[30] B. L. Mbanga, F. F. Ye, J. V. Selinger, R. L. B. Selinger, *Phys. Rev. E* **2010**, *82*, 4.
[31] Additionally, an experiment was carried out in which a strip was cut from a two-domain alternating film at a 45 degrees angle.[23] Based on previous research, we predicted a deformation into a coiled shape, with a left-handed coil on one side and a right-handed coil on the other side of the strip. Upon heating the film, this deformation was indeed observed. Finite element simulation of this actuator agrees with the experimental observation (see Supporting Information).
[32] C. Ohm, E. Fleischmann, I. Kraus, C. Serra, R. Zentel, *Adv. Funct. Mater.* **2010**, *24*, 4314.
[33] H. Yang, A. Buguin, J. Taulemesse, K. Kaneko, S. Méry, A. Bergeret, P. Keller, *J. Am. Chem. Soc.* **2009**, *131*, 15000.
[34] Salome, an open source Q4tool downloaded from http://www.salome-platform.org (last accessed: October 2013).